Experimental Comparison of Slow and Fast Gas Heating Processes to Reduce the Deflagration-to-Detonation Run-up Distance in Hydrogen-Air Detonations

Mhedine Alicherif and Deanna A. Lacoste
Clean Energy Research Plateform, King Abdullah University of Science and Technology (KAUST)
Mechanical Engineering Program, Physical Science and Engineering Division, KAUST
Thuwal 23955-6900, Saudi Arabia

1 Introduction

Detonation represents the supersonic propagation mode of combustion waves, characterized by high pressure and temperature behind the propagating shock front. These conditions make detonation particularly suitable for propulsion applications, such as pulsed detonation engines [1] and rotating detonation engines [2], as well as power generation systems [3]. A key challenge in utilizing detonation is achieving a self-sustained state under Chapman-Jouguet (CJ) conditions over short distances and with minimal input energy. The most employed strategy to initiate detonation is the deflagration-to-detonation transition (DDT) process. Although deflagration waves are inherently unstable and will accelerate to create the conditions necessary for DDT, this process can be significantly enhanced using geometric arrangements or obstacles, which induce turbulence along the deflagration path. However, these obstacles introduce design complexity and are prone to degradation over time. Therefore, exploring alternative approaches to achieve efficient DDT remains an important area of investigation.

Plasma-assisted combustion has been extensively studied over the past two decades, with recent reviews [4, 5] highlighting its impact on energy branching in combustible mixtures and reduced activation energy. Nanosecond discharges are particularly effective due to their ability to quickly input energy, leading to high molecular dissociation [5], fast gas heating (FGH) [6], and compression waves [7]. Compared to thermal plasmas, nanosecond discharges enable faster and shorter DDT transitions. Studies by Zhukov et al. [8] and Alicherif et al. [9] demonstrated reduced DDT times for hydrocarbons and hydrogen mixtures using high-voltage nanosecond discharges over conventional spark plugs. Gray et al. [10] reported significant reductions in DDT run-up length with nanosecond repetitive pulses (NRP), while Tropina et al. [11] showed numerically that oxygen dissociation via nanosecond discharges is more effective than thermal plasma Joule heating for DDT. However, Vorenkamp et al. [12] observed a nonlinear relationship, with longer nanosecond discharges leading to extended DDT transition lengths in microchannels showing that there are still non-trivial interactions of plasma actuation and DDT.

This study investigates the difference in DDT run-up distance for the same deposited energy between discharges that primarily excite molecules, leading to slow gas heating, and those that excite atoms and ions, resulting in fast gas heating.

Correspondence to: mhedine.alicherif@kaust.edu.sa

2 Experiemtal Setup and methods

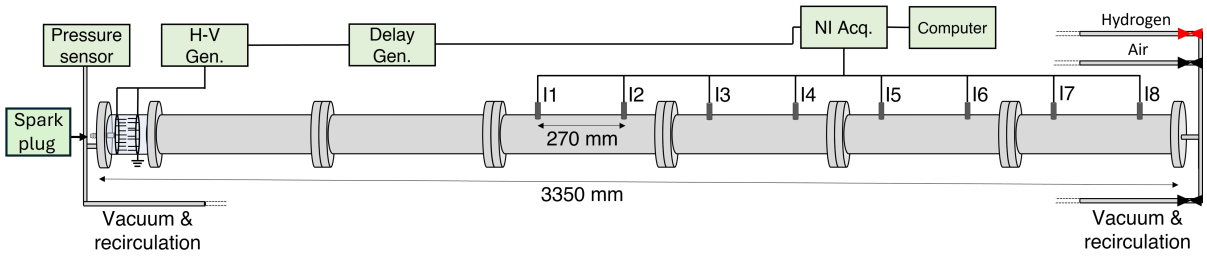

Figure 1: Experimental setup. H-V Gen= High Voltage Generator, Delay Gen.= Delay Generator, NI Acq.= National Instrument Acquisition system.

A schematic of the experimental setup is shown in Fig.1. The deflagration tube, made of stainless steel, is 3350 mm long with a diameter of 39 mm. It consists of six independent stainless steel sections and one movable glass section.

The fuel-air mixture used is stoichiometric H_2:Air, prepared via the partial pressure method and monitored by a static pressure gauge (Keller Leo 3). Experiments are conducted at 1 bar and ambient temperature. Prior to each experiment, the tube is flushed with compressed air to remove impurities, and a vacuum of 0.1 mbar is achieved using a vacuum pump (Edward RV8). After fuel and air injection, the mixture is recirculated for three minutes using a recirculation pump (KNF Laboport N 842.3 FT.18).

Eight ionic probes, spaced 270 mm apart, are positioned to detect voltage drops caused by ions in the flame front. The signals are recorded by a high-speed acquisition system (NI PXI-5105 Oscilloscope), enabling real-time characterization of the combustion front's instantaneous speed. This parameter is used to determine whether the deflagration has transitioned to a detonation.

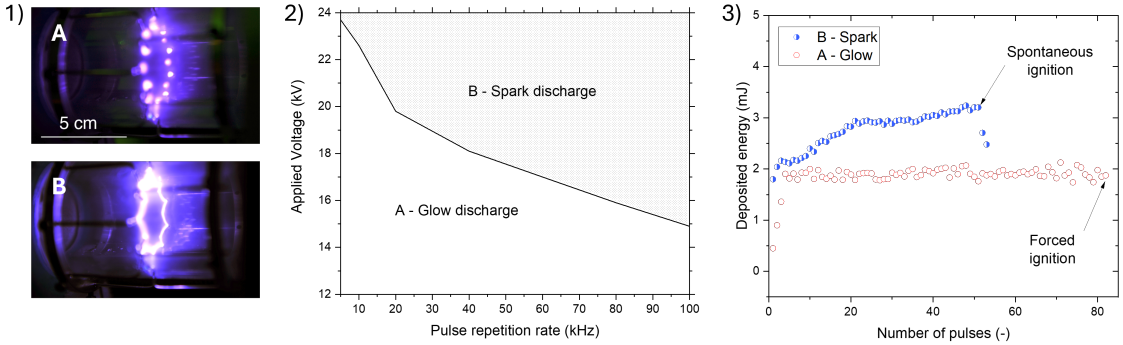

Figure 2: Discharge characteristics: 1) pictures of the discharge in the Glow and Spark regimes 2) Parametric plot for A and B 3) Total number of pulses to achieve the same deposited energy.

The high voltage electrodes are installed in the glass section and powered by a Nanosecond Repetitive Pulsed (NRP) discharge generator (FID FPD 25-100MC2). The voltage amplitude is varied between 2 kV and 12.5 kV, while the repetition rate is adjusted from 5 to 100 kHz to control the discharge characteristics. In this study, two discharges are investigated, as shown in Fig. 2. Figure 2-1) illustrates the discharge in the first mode, "A - Glow Discharge," where no noticeable gap closure occurs between the electrodes, and in this case, relatively low and slow heating is expected. In contrast, the second mode, "B - Spark Discharge," is characterized by a visible gap closure, potentially leading to fast and high

heating. The transition between these modes can be easily achieved by slightly increasing the applied voltage while keeping the pulse repetition rate constant, as shown in Fig.2-2).

To ensure a fair comparison between the two regimes, the number of pulses for each condition was selected to achieve similar energy deposition. In the spark regime, the number of pulses required for spontaneous ignition (due to temperature increase) was recorded at 100 kHz and 17 kV, corresponding to 55 pulses and approximately 150 mJ of deposited energy. For the glow discharges, enough pulses were applied to reach a similar energy deposition of around 150 mJ, which required 90 pulses at 100 kHz and 15 kV. Once this energy threshold was reached, ignition was initiated by an independent spark plug located near the electrodes. It is important to note that the energy from the spark plug was not included in this study.

3 Results and discussion

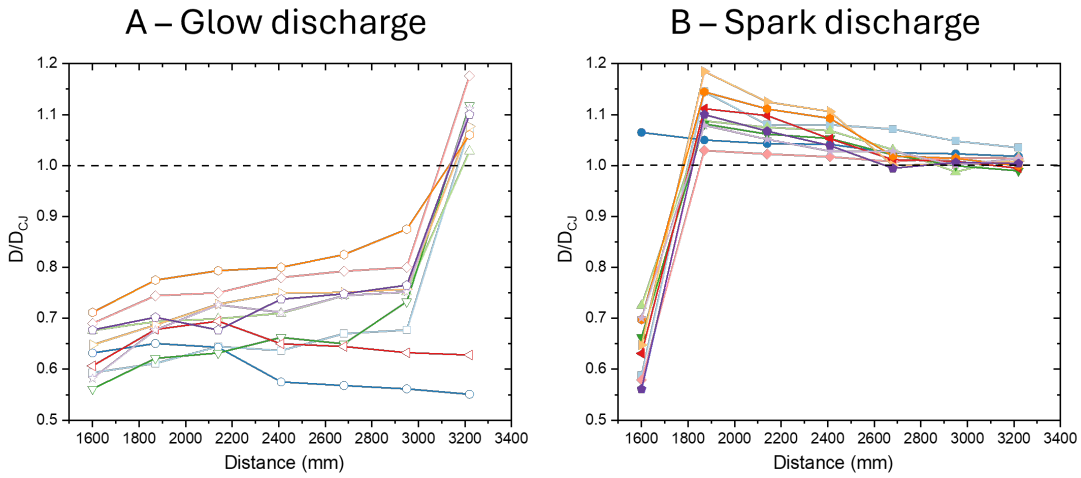

Figure 3: Flame acceleration and transition to detonation recorded by ionic probes over ten shots for the cases: A - Glow Discharge, and B - Spark Discharge.

Figure 3 shows the flame speed profiles for no plasma, the glow discharge, and the spark discharge. Note that, in the absence of plasma, no transition to detonation is observed, the flame continues to accelerate without transitioning [10]. With the glow discharge, the flame speed increases slightly, and detonation is typically observed at the end of the tube. For the spark discharge, detonation occurs at a shorter distance, around 1.8 m in most cases, with some instances of transition occurring even earlier, before the first ionic probe. This indicates that the spark discharge significantly enhances the DDT process. In contrast, while DDT is achieved with the glow discharge, it only occurs near the tube's end.

We aim to explain the presented results through spectroscopy by examining the different heating mechanisms induced by the reduced electric field in the plasma. Optical emission spectra for both discharges in air were recorded in the ultraviolet (UV) range (275–435 nm) using a spectrometer (Princeton Instruments, Acton SP2750) of 750 mm focal length equipped with an ICCD camera (PIMAX-4). The spectra were time-resolved to analyze each pulse individually. Comparing the relative intensities of the bands allows us to evaluate the population of excited levels, particularly for N_2 and N_2^+, and to estimate the temperatures and reduced electric field.

Figure 4 shows the spectra obtained in the regions of interest, 350–358 nm and 390–396 nm. For the glow discharge, the emission is primarily dominated by molecular N_2 bands, suggesting that the dis-

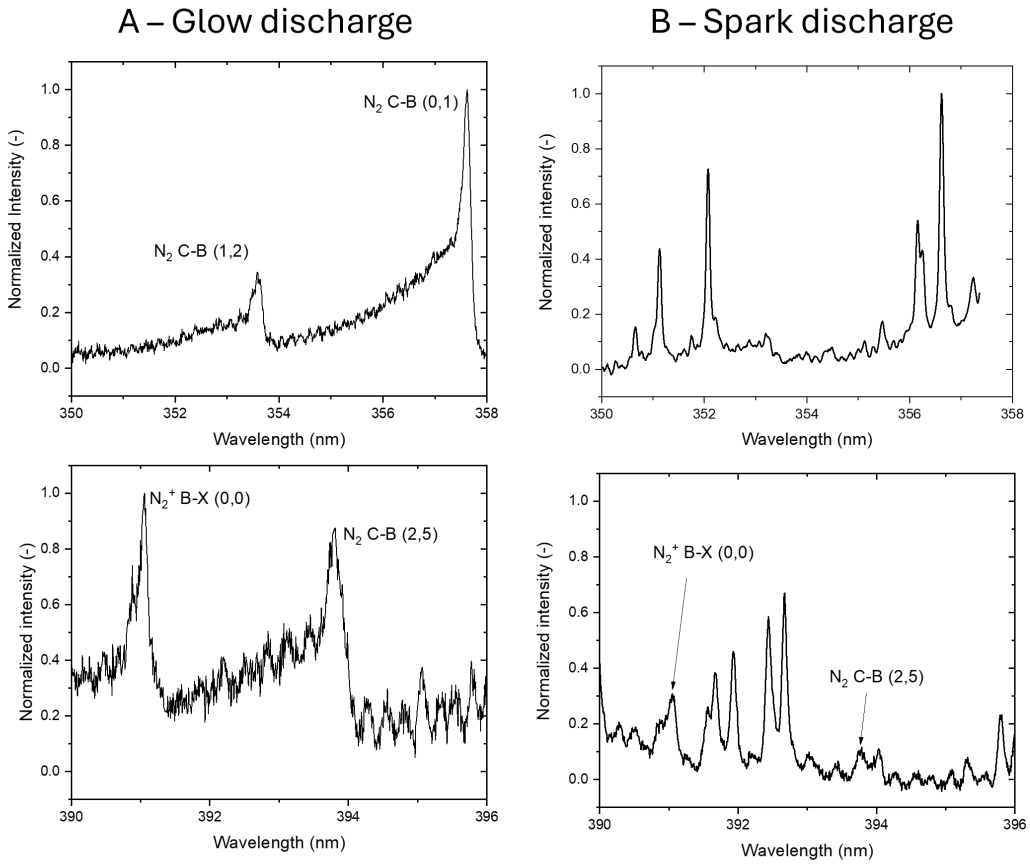

Figure 4: Emission spectra for the glow and spark discharge between 350-358 nm and 390-396 nm.

charge chemistry is mainly driven by molecular excitation, leading to slow relaxation and subsequent gas heating. The spectrum in the 350–358 nm range can be theoretically fitted to estimate the vibrational temperature of N_2 as well as the rotational/translational temperature. A significant discrepancy is observed between the vibrational temperature (T_{vib} = 3200 ± 320 K) and the rotational temperature (T_{rot} = 1700 ± 170 K), indicating incomplete relaxation of the vibrational levels. In contrast, for spark discharge, the emission is dominated by atomic and ionic lines, suggesting that the chemistry is mainly ionization and dissociation, leading to short-lived excited species. However, the molecular bands in the 350–358 nm range are no longer detectable due to experimental noise, making it impossible to fit the spectrum.

The reduced electric field in the plasma (E/N) can be estimated by comparing the intensities of two lines at 391 nm for $N_2^+(B^2\Sigma_u^+ \rightarrow X^2\Sigma_g^+)$ and 394 nm for $N_2(C^3\Pi_u \rightarrow B^3\Pi_g)$, following the work of Paris et al. [13]. The intensity ratio $R_{391/394}$ is given by:

$$R_{391/394} = 46 \exp\left(89 \left(\frac{E}{N}\right)^{-0.5}\right) \tag{1}$$

where $R_{391/394}$ is the ratio of the intensities of the 391-nm and 394-nm lines, and E/N is the reduced electric field in Townsend. This method was proposed and validated for air plasmas [13], where nitrogen molecules are predominantly excited from the ground state by direct electron impact, which is the case of our study. The estimated reduced electric field for the glow discharge was $E/N = 480 \pm 60$ Td, while

for the spark discharge it was 990 ± 100 Td. These estimates can be correlated with the calculated energy loss fraction for the mixture, as shown in Fig. 5. The energy loss fraction is determined using Bolsig+ by computing the fraction of electron energy lost through inelastic collisions, including excitation and ionization, relative to the total energy input. The collision cross-sections were obtained from Phelps database [14] for this mixture.

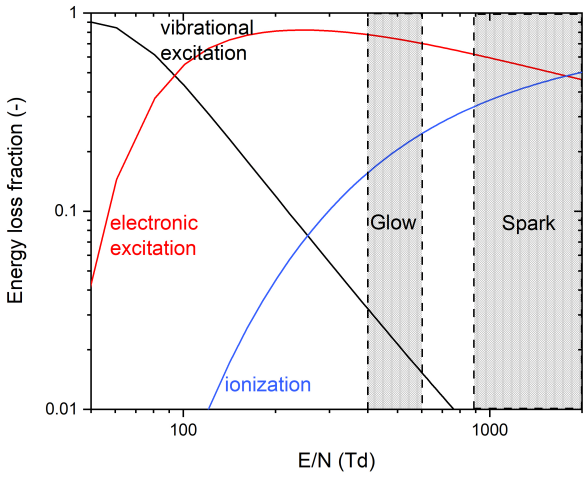

Figure 5: Calculated Energy loss fraction in the discharge for the H_2:Air mixture.

Figure 5 illustrates that, for glow discharge, the dominant process is the electronic excitation of the molecules. Note that both the nondissociative and dissociative electronic excitations are merged, but for high values of reduced field the collision becomes dissociative. That is why for spark discharge, dissociative excitation, and ionization dominate. These processes result in rapid gas heating because of the relaxation of short-lived species. The sharp temperature rise generates localized shockwaves, creating highly turbulent flows that are ideal for flame acceleration. Schlieren images will be presented in the extended version of this work to further validate these findings.

4 Conclusion

This study highlights the significant impact of discharge mode on the deflagration-to-detonation transition (DDT). The glow and spark discharges were studied under comparable energy deposition conditions, with their effects analyzed using ionic probe measurements for the speed of the front, and time-resolved spectroscopy to understand the plasma effects.

The spark discharge, characterized by rapid gas heating through ionization and dissociation processes, drastically reduces the DDT run-up distance compared to the glow discharge, where molecular excitations dominate. Spectroscopic analysis confirmed higher reduced electric fields and distinct energy deposition mechanisms for each mode, with the filamentary discharge generating localized turbulence through shockwaves. These findings emphasize the potential of fast gas heating to enhance DDT in practical applications.

5 Acknowledgments

This study was funded by the King Abdullah University of Science and Technology, through the baseline fund BAS/1/1396-01-01.

References

[1] Kailasanath, K. (2000). Review of propulsion applications of detonation waves. AIAA journal, 38(9), 1698-1708.

[2] Wolański, P. (2013). Detonative propulsion. Proceedings of the combustion Institute, 34(1), 125-158.

[3] Rasheed, A., Furman, A. H., and Dean, A. J. (2011). Experimental investigations of the performance of a multitube pulse detonation turbine system. Journal of Propulsion and Power, 27(3), 586-596.

[4] Starikovskiy, A., and Aleksandrov, N. (2013). Plasma-assisted ignition and combustion. Progress in Energy and Combustion Science, 39(1), 61-110.

[5] Ju, Y., and Sun, W. (2015). Plasma assisted combustion: Dynamics and chemistry. Progress in Energy and Combustion Science, 48, 21-83.

[6] Popov, N. A., and Starikovskaia, S. M. (2022). Relaxation of electronic excitation in nitrogen/oxygen and fuel/air mixtures: fast gas heating in plasma-assisted ignition and flame stabilization. Progress in Energy and Combustion Science, 91, 100928.

[7] Takashima, K., Zuzeek, Y., Lempert, W. R., and Adamovich, I. V. (2011). Characterization of a surface dielectric barrier discharge plasma sustained by repetitive nanosecond pulses. Plasma Sources Science and Technology, 20(5), 055009.

[8] Zhukov, V. P., Rakitin, A. E., and Starikovskii, A. Y. (2008). Effect of high-voltage pulsed discharges on deflagration to detonation transition. Journal of Propulsion and Power, 24(1), 88-93.

[9] Alicherif, M., Lafaurie, V., Claverie, A., Starikovskaia, S., and Vidal, P. (2022, June). Detonability enhancement by use of a nanosecond plasma. In 28th International Colloquium on the Dynamics of Explosions and Reactive Systems.

[10] Gray, J. A., and Lacoste, D. A. (2019). Enhancement of the transition to detonation of a turbulent hydrogen–air flame by nanosecond repetitively pulsed plasma discharges. Combustion and Flame, 199, 258-266.

[11] Tropina, A. A., and Mahamud, R. (2022). Effect of plasma on the deflagration to detonation transition. Combustion Science and Technology, 194(13), 2752-2770.

[12] Vorenkamp, M., Steinmetz, S. A., Chen, T. Y., Mao, X., Starikovskiy, A., Kliewer, C., and Ju, Y. (2023). Plasma-assisted deflagration to detonation transition in a microchannel with fast-frame imaging and hybrid fs/ps coherent anti-Stokes Raman scattering measurements. Proceedings of the Combustion Institute, 39(4), 5561-5569.

[13] Paris, P., Aints, M., Valk, F., Plank, T., Haljaste, A., Kozlov, K. V., and Wagner, H. E. (2005). Intensity ratio of spectral bands of nitrogen as a measure of electric field strength in plasmas. Journal of Physics D: Applied Physics, 38(21), 3894.

[14] Phelps database, www.lxcat.net, retrieved on January 10, 2025.